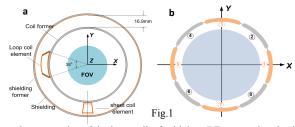# Modelling Study of a Hybrid Loop-Sheet Coil Structure for a 8-channel Small Animal Transceive Array at 9.4T

Y. Li[1], F. Liu[1], J. Jin[1], E. Weber[1], B. Li[1], and S. Crozier[1]
[1]School of ITEE, The University of Queensland, Brisbane, QLD, Australia
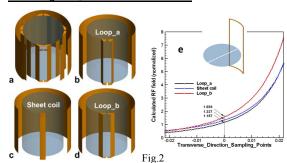
Introduction   When designing a small animal RF transceive array coil, RF field penetration depth and mutual decoupling of individual coil elements are two important considerations. Conventionally, loop coils are used for the construction of small animal transceive arrays. However, as the number of coil elements increases the size of each coil has to be reduced, since the available space is generally restricted, to comply with MRI-system specifications. As a result the RF penetration depth will be compromised. In this work, a 9.4T shielded 8-channel hybrid loop-sheet coil transceive array for small animal MRI is proposed to overcome the low RF penetration depth issue.

Methodology   The major constraint when designing the small animal 8-channel transceive array is the limited available space to accommodate the coil elements and decoupling circuits. In our previous studies, a loop coil-element with angularly-oriented radiating structures was presented which was capable to increase the RF penetration depth and to regulate the mutual coupling between neighbouring coils [1-2]. However, the opening angle of the loop aperture is limited to 35º (see Fig.1a and Fig.2b) [1], which is one of the limiting factors for further improvement of the RF field penetration depth. To overcome this constraint, we investigated a combination of sheet coil element [3-4] and angularly-oriented loop element. Illustrated in Fig.1b is the coil element diagram of the new design (transverse view). Angularly-oriented loop coils are used at positions 1, 3, 5 and 7, while sheet coils are used at locations 2, 4, 6 and 8. This hybrid
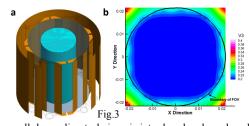

Fig.1

loop-sheet coil design provides a higher degree of freedom to optimize the coil blade rotation angle and aperture size of the loop coils, for highest RF penetration depth and minimum mutual coupling between neighbouring coils.
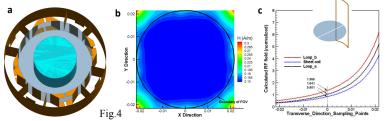
Modelling Study and Simulation Results

Fig.2

Shown in Fig.2a is the modelling of the proposed hybrid coil. Depicted in Fig.2d is the optimized loop coil element. The opening angle of the loop aperture was increased to 45º considering physical constraints. In addition, when using the numerical optimization algorithm, the optimum coil blade rotation angle of 20° was obtained. Using a hybrid MoM/FEM simulation package (FEKO), a comparison of RF field penetration depth between **Loop_a** (previous design, Fig.2b), sheet coil element (Fig.2c) and **Loop_b** (Fig.2d) was undertaken. All the modelled coil elements are excited with a voltage source of 1V and a 0º phase, tuned to 400MHz and matched to 50Ω. Magnetic fields inside the FOV (transverse to the region of interest) are calculated and plotted in Fig.2e. It is shown that the calculated magnetic field at the centre of the FOV (as depicted in the sub-figure of Fig.2e) for the sheet coil element is approximately 14.7% higher than that of **Loop_a**, and **Loop_b** is approximately 34.66% higher, as compared to **Loop_a**. These results demonstrate the potential of the proposed new design.

Mutual coupling problems always accompany the design of phased arrays. Two decoupling methods are proposed to resolve the mutual coupling effect of the hybrid loop-sheet coil design. First, a counter-wound inductor decoupling method [1], as shown in Fig.3a, is tested. A homogenous cylindrical phantom (43.2mm in diameter and 90mm in length, $\sigma = 0.01$ S/m and $\varepsilon_r = 2.72$), was modelled for loading purposes. With the appropriate interlacing area and distance between the decoupling inductors, isolation of -24dB between coils can be obtained. The magnetic field inside the cylindrical phantom, on the transverse section, with the decoupled coil elements excited in a birdcage-like mode (simultaneous excitation of all the decoupled coil elements with voltages sources of 1V but with 45° phase shift individually) was calculated and shown in Fig. 3b.

Fig.3

Fig.4

Second, an isolation wall decoupling technique is introduced and employed to decouple the coil. As shown in Fig.4a, this decoupling method acts as an isolation wall between the coil elements. In this case, each coil element is isolated by the wall and works independently in a chamber. Being part of the RF shield, the isolation wall between the coils is employed to minimize leakage flux between the neighbouring coil- elements, and concurrently steer the flux closer to the sample. Isolation of -22dB between coils can be obtained through adding the isolation wall. Similarly, magnetic field inside the phantom was calculated and shown in Fig.4b.

Although the isolation wall can provide high decoupling power, the RF field penetration is reduced as compared to the counter-wound inductor decoupling method. Because the isolation wall forms part of the shield, each coil element is now closer to the shield and, theoretically, this will reduce the coil efficiency. A comparison study was undertaken and the effective RF penetration for these three coil elements is plotted in Fig.4c. Under loaded conditions, at the centre of the cylindrical phantom, with the current design, the RF penetration of the **Loop_b** can be increased (approximately 31.4%), while a decline is noticed for the sheet coil element (approximately 18.3% reduction) compared to the **Loop_a** (using the counter-wound inductor decoupling method).

Conclusion   In this work, a dedicated 9.4T 8-channel hybrid loop-sheet coil transceive array for small animal MRI is modelled and studied. The array was designed within the limited space available by using a dedicated coil structure that contains loop and sheet coil elements. The hybrid design enables large aperture for the loop coil, therefore offering improved RF field penetration and coil efficiency. By using numerical modelling/simulation, we were able to determine the feasibility of the hybrid-designed and also understand its performance and field behaviour.

References
[1] Weber *et al*, IEEE EMBS, pp. 2039-2042, 2008. [2] Weber *et al*, ISMRM, pp. 151, 2008. [3] Ullmann *et al*, Mag. Res. Med., 2005. 54(4): p. 994-1001. [4] Lee *et al*, Mag. Res. Med., 2001. 45(4): p. 673-683.